International Forum on Aeroelasticity and Structural Dynamics
IFASD 2024
17-21 June 2024, The Hague, The Netherlands

ON THE AEROELASTICITY OF HIGH ASPECT RATIO STRUT-BRACED WINGS: A PARAMETRIC STUDY – IFASD 2024

Hamad Almarzooqi[1], **Rafic Ajaj**[1], **Wesley Cantwell**[1]

[1]Khalifa University of Science and Technology
Shakhbout Bin Sultan St, Hadbat Al Za'faranah, Zone 1, Abu Dhabi
100062577@ku.ac.ae
rafic.ajaj@ku.ac.ae
Wesley.cantwell@ku.ac.ae

Keywords: Aeroelasticity, High Aspect Ratio, structural dynamics, Strut-braced wing

Abstract: The aviation industry is increasingly adopting high aspect ratio (AR) wings to meet the demands for more efficient and emission-friendly aircraft. High AR wings increase aerodynamic efficiency but come at the cost of structural and aeroelastic issues. A candidate solution for these aeroelastic issues is strut-bracing. This paper conducts a comprehensive parametric study on a high aspect-ratio (AR = 16) strut-braced flat plate to identify the influence of material and geometric parameters on structural performance and aeroelastic stability. The finite element method is used for structural modelling, the doublet lattice method for aerodynamic modelling, and an infinite plate spline for aero-structural coupling. The analysis is conducted using MSC Nastran and MATLAB. The geometric variables include the location of the strut on the plate, the location of the strut on the fuselage, and boundary conditions on strut ends. The material of the plate is then changed from Aluminum-2024 to Carbon Fibre Reinforced Plastic composite, and the ply orientation and layup are also varied. The location of the strut on the plate is varied chordwise and spanwise, while the location of the strut on the fuselage is either fixed at mid-chord or variable with the location of the strut on the wing. The boundary conditions on the strut end (fuselage-wing) are varied between clamped and pinned (4 combinations). The optimum geometric parameters for the metal plate are found to be clamped-integral boundary conditions, with the variable location on the fuselage. The optimum geometric parameters are applied to the composite plate, and the ply orientation and strut location on the plate are studied. The optimum has a ply layup of $[0, 45°]s$, and a strut location at 20-30% of the span, and 30-50% of the chord. This results in a 37% increase in the critical speed, a 71.5% decrease in the max bending moment and 21.35% decrease in shear forces.

1 INTRODUCTION

Demand in commercial aviation is continuously rising [1], resulting in a need for more efficient aircraft. A trend in increasing the aspect ratio of the wing to increase aerodynamic efficiency is becoming prevalent in recent aircraft design progressions [2]. This comes at the cost of structural flexibility, resulting in increased weight and possible aeroelastic instabilities [3] [4] [5]. One way to solve this issue is by strut-bracing of the wing [6] [7] [8]. There is a lack of a comprehensive parametric study in the literature around the strut-braced high-aspect ratio wing, which this paper aims to provide.

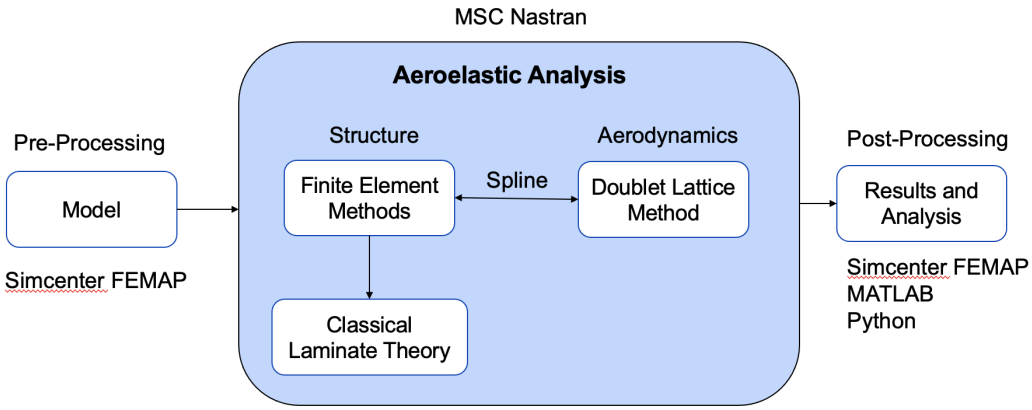

Figure 1: Methodology Chart

2 METHODOLOGY, MODEL AND LOAD CASE

Numerical methods are used for the aeroelastic analysis in this paper. FEMAP is used to build the structure and the aerodynamics model and for splining them. MSC Nastran [] is used to conduct the static and dynamic aeroelastic analysis. The structure is modelled using finite element methods [9], mainly the CQUAD4 plate element. The aerodynamics is modelled using the Doublet Lattice Method [10]. Classical Laminate Theory is used for the composite material modelling. Post-processing of results is done using Femap and Matlab. Plotting is done using python Matplotlib. Figure 1 summarizes the methodology of this paper.

A strut-braced flat plate is utilized for the aeroelastic analysis as a simplified representative model of a high aspect ratio strut-braced wing. The flat plate has an aspect ratio of 16, a span of $4m$ and a chord of $0.25\,m$. One end of the strut is positioned at $0.4\,m$ below the root of the wing, and the other end is connected at the wing using a rigid element to avoid stress concentrations. Different spanwise and chordwise locations of where the strut connects to the wing are considered. This is a rib that exists at the strut connection of an actual wing. Figure 2 displays the top and side views of the strut-braced flat plate including the rigid element. The black circle at the root depicts a clamped boundary situation of the wing root, while the white circle denotes varying boundary conditions that are altered during the analysis. The flat plate has a thickness of $5\,mm$, and the strut is straight with a width of $25\,mm$ and a height of $2.5\,mm$.

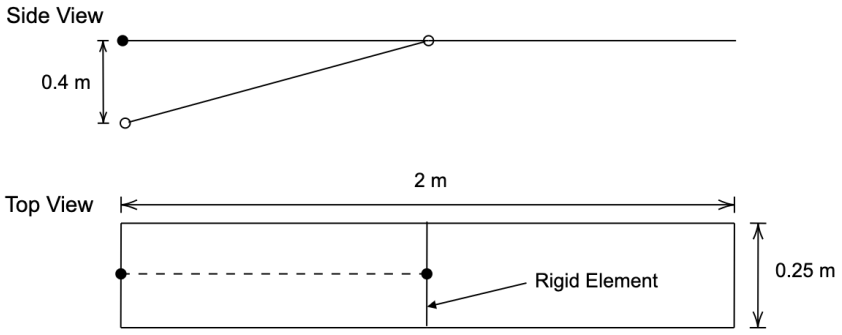

Figure 2: Side and Top View of the Flat Plate Model

A benchmark study is conducted using an aluminium flat plate without a strut to compare findings and characteristics. The dynamic analysis of the benchmark study results in an instability

(flutter) velocity of $53\,m/s$. To ensure safety, a 20% safety margin is employed, and a small angle of attack is introduced. This aids in the formation of the load case for the static analysis. The load case parameters are presented in table 1.

Table 1: Load Case

Property	**Value**
Angle of Attack	3°
Dynamic Pressure	$551.25\,Pa$
Density	$1.225\,kg/m^3$
Speed	$30\,m/s$

Static analysis of the reference case under the conditions described in table 1 is done, and the resulting structural parameters are used to compare all results of geometric and material variations of the strut-braced flat plate. Essential benchmark parameters are described in table 2.

Table 2: Reference Case Benchmark Structural Parameters

Property	**Value**
Critical Speed	$53\,m/s$
Shear Force	$-97.47\,N$
Bending Moment	$-93.1\,Nm$
Tip Deflection	$0.4716\,m$
Tip Twist	1.097°
Max Von-mises Stress	$89.4\,MPa$

Aluminum 2024 alloy is employed as the material for this analysis. Information regarding the essential properties of the material can be found in Table 3.

Table 3: Al-2024 Properties

Property	**Value**
Modulus of Elasticity	72 GPa
Poisson's Ratio	0.3
Shear Modulus	27.69 GPa
Density	2700 kg/m^3

2.1 Convergence Study

A mesh convergence analysis is conducted on both the structural and aerodynamic meshes to validate the accuracy of the model. The mesh size is determined by the number of chord-wise elements on the flat plate. This involves comparing the lift generated using different aerodynamic mesh sizes. The mesh size is determined by the number of elements chord-wise on the aerodynamic panel, which is similar to the structural mesh convergence study. Figure 3 illustrates the lift for different mesh sizes. A mesh size of 10 elements in the chord-wise direction is deemed adequate in providing reliable lift results while maintaining computational efficiency. A similar study on the structural mesh natural modes shows that 10 chord-wise elements also yields satisfactory accuracy at low computational cost.

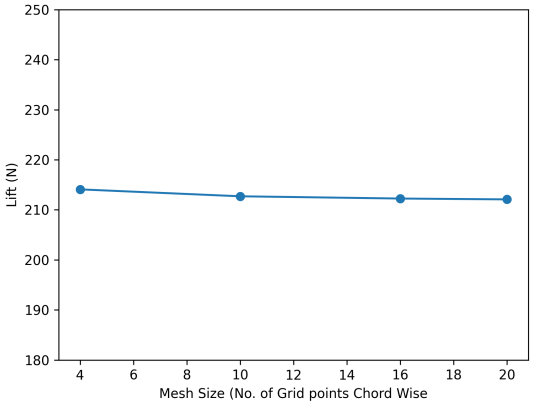

Figure 3: Aerodynamic Mesh Convergence Study

2.2 Design variables

This section of the study compares the effect of geometric variables of the strut on the aeroelastic properties of the system. The geometric variables fall under three categories: strut location on the wing, strut location on the fuselage, and strut boundary conditions. The effect of the material and geometric variables of the strut will be studied later on.

2.2.1 A. Boundary Condition of The Strut

The connection of the strut to the fuselage and the wing are also varied. For the end of the strut at the fuselage, two connection types have been considered (clamped and pinned). Similarly, the end of the strut at the wing, two connection types have been considered (integral and pinned). This results in 4 combinations. Figure 4 illustrates the connection types.

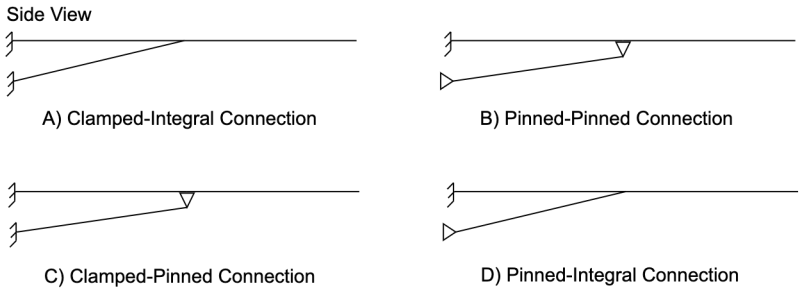

Figure 4: Combinations of Strut Boundary Conditions

2.2.2 B. Strut Location on Fuselage

The location of the strut on the fuselage is also varied in two cases. In the first case, the strut is fixed to a location on the fuselage that is at the mid-chord. The second case has the strut location on the fuselage vary with its location on the wing. Figure 5 depicts the two cases and showcases the strut being angled and straight when seen from above.

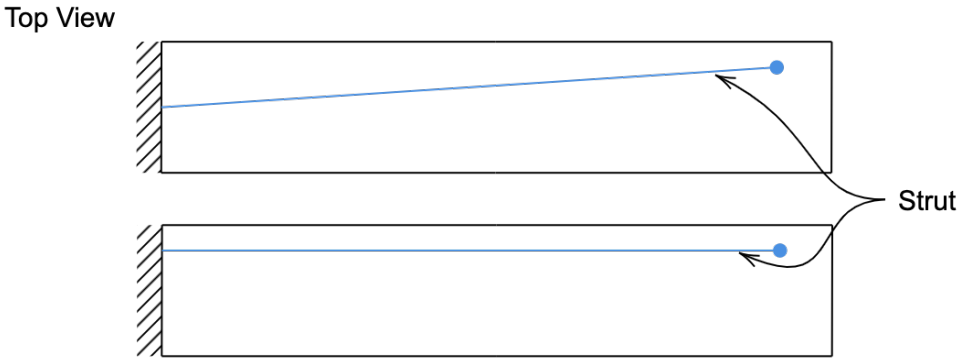

Figure 5: Strut Location on Fuselage (Top is Fixed at Mid-Chord, and bottom matches the location on the wing)

2.2.3 C. Strut Location on Plate

The location of the strut connection to the wing is varied along the span and the chord. There are 10 possible locations chordwise, varying from the leading edge to the trailing edge in 10% increments. Likewise, there are 10 possible locations spanwise, varying from 10% of the span to the full length of the plate. This results in 100 possible locations for the strut to connect to the wing.

2.2.4 D. Ply Orientation of Composite Laminate + Strut Location

The geometric optimum variables will be used as a starting point for the composite plate analysis, then the material of the flat plate will be composite CFRP and the ply orientation and strut location will be varied together. For the sake of fair comparison, the mass of the metallic plate and that of the composite plate are kept the same. This implies that the thickness of the compos-

ite plate is $7.5\,mm$ (it was $5\,mm$ for the metallic flat plate). The rationale behind keeping the mass of the metallic and composite plates the same is to expand the operational flight envelope for a given mass.

Table 4: CFRP Properties [11]

Property	Value
Longitudinal Elastic Modulus, E1	129 GPa
Transverse Elastic Modulus, E2	9 GPa
Shear Modulus	3.4 GPa
Poisson's Ratio	0.34
Density	1800 kg/m^3

Composite materials are gaining popularity in the aerospace industry. The material used in the composite plate is Carbon Fibre Reinforced Plastics (CFRP), the essential properties are shown in table 4 [11]. The material of the strut is not changed and remains Al-2024 metal.

The material of the plate is included as a variable to be studied. The Laminate is made of 4 plies each of a thickness of $1.875\,mm$. The ply orientation is varied in this parametric study to maximize favourable aeroelastic tailoring. The laminate is symmetric and unbalanced, and had the orientation $[0, \theta]_S$, where θ is variable. The orientation of θ is defined with respect to the material coordinate system, which differs from the model coordinate system as shown in figure 6, and respective ply orientations are also shown. The composite plate is also modelled using CQUAD4 element in MSC Nastran.

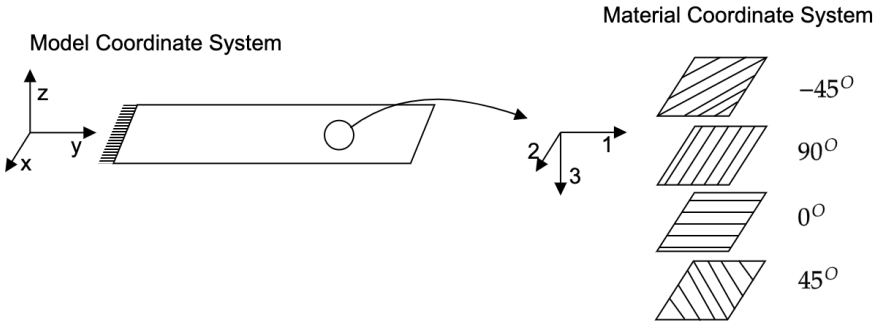

Figure 6: Model and Material Coordinate Systems

The strut location is varied in the same way as discussed in the previous section, with a 100 total possible locations encompassing the entire plate. It should be noted that the composite strut is not considered in this parametric study because initial investigation showed that composite strut offers little performance improvement, while increasing the complexity of the study and the number of design variables.

3 RESULTS

3.0.1 A. Boundary Condition of The Strut

The first analysis compares the results of different boundary conditions of the strut's connections. Figure 7 shows the max von-mises stress on the plate for different strut's locations for different boundary condition. This allows for the selection of the optimum case that reduces structural loads. It is evident from figure 7 that the boundary condition has little effect on the sresses acting on the plate. Cases that have a pinned boundary condition at the strut-to-wing

joint have marginally less viable locations (0-10% of the span and 80-100% of the chord). Clamped-Integral and Pinned-Integral cases are almost identical, with Clamped-Integral being slightly better. Thus, the clamped-integral case is the optimum boundary condition because it offers higher reduction in the von-mises stresses across the plate.

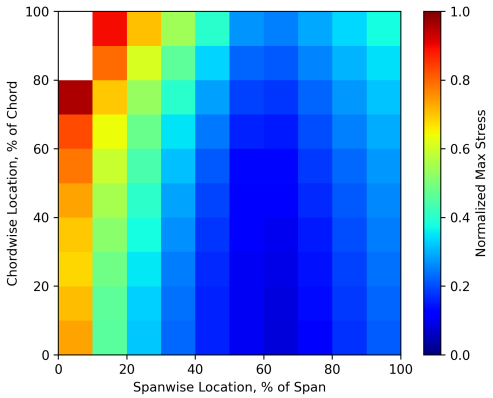

(a) Clamped-Integral

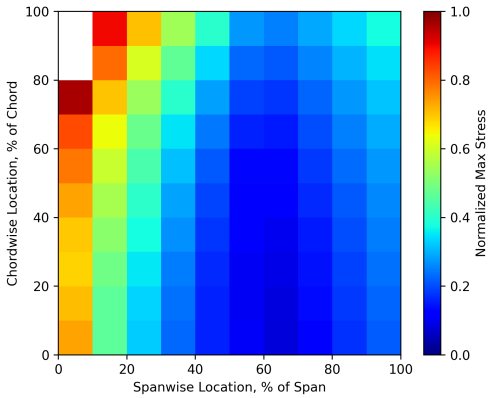

(b) Pinned-Integral

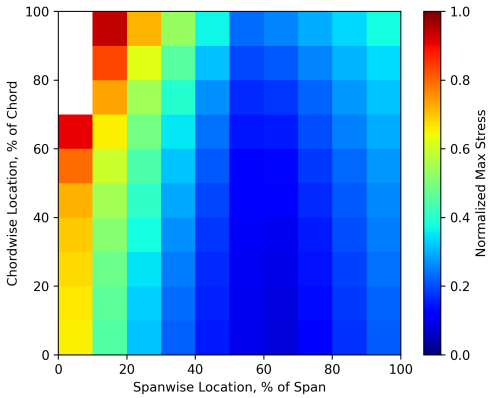

(c) Clamped-Pinned

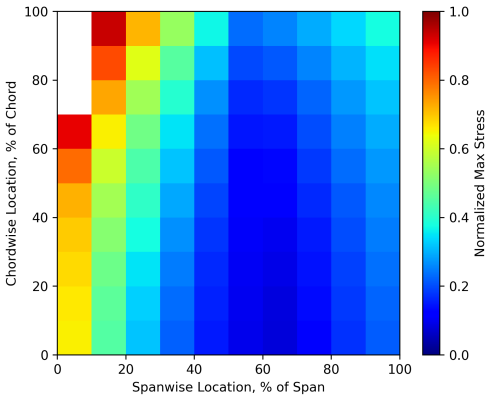

(d) Pinned-Pinned

Figure 7: Max Von-Mises Stress on the Plate by strut Location for different boundary condition cases

3.0.2 B. Strut Location on Fuselage

The strut location on the fuselage is varied in the chordwise direction. Figure 8 depicts the max stress on the plate of both variations (variable and fixed strut locations on fuselage). Figure **??** depicts max stresses on the strut for both variations as well.

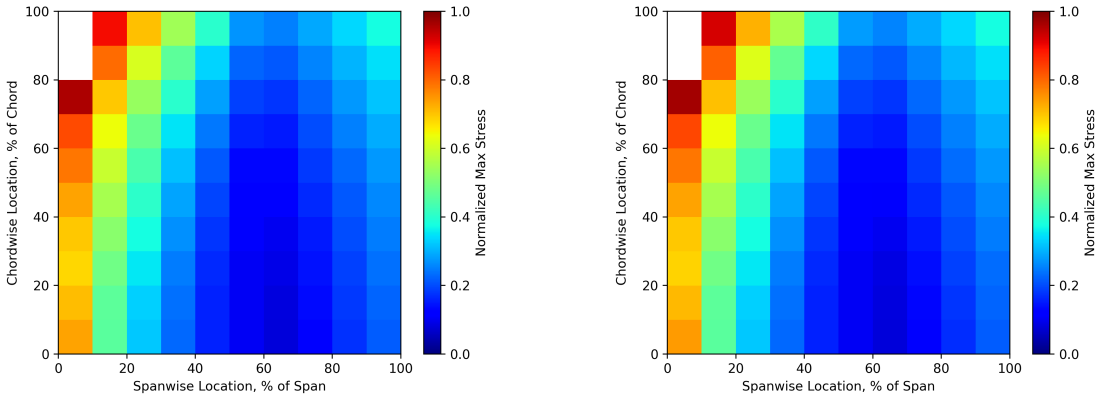

(a) Strut Variable on Fuselage

(b) Strut Fixed on Fuselage

Figure 8: Max stress by strut location for variable and fixed strut location on fuselage

Similar to the boundary condition variable, there is no significant difference. However, the variable strut location case has slightly better performance. Moreover, a variable strut location on the fuselage allos for a shorter and lighter strut. This is preferable as it will reduce the weight and aerodynamic effect of the strut.

3.0.3 C. Strut Location on Plate

The root shear force and bending moment values are not representative of their respective maximum values, and as such, a spanwise analysis of shear force and bending moment of each strut locatin case has to be done. As it is no longer a cantilever configuration, the bending moment and shear force are no longer maximum at the root of the plate. Spanwise shear force and bending moment for an example case where the strut is at mid-span mid-chord location are shown in Figure 9. It can be seen that the maximum bending moment and shear forces occur at the strut location in this case. This effect is similar to the effect of the engine weight on the shear and bending moment distribution of the wing, although it is much more pronounced in this case.

Analysis of strut location on the wing is done on the clamped-integral case with a variable strut location on the fuselage. Figure 10 shows the normalized max bending moment and shear force at each strut location considered.

The normalized bending moment plot shows improvements at all strut locations. Locations near the trailing edge, at a region close to the root of the flat plate, provide slight improvements in structural performance. A strut location towards the mid-span and leading edge of the flat plate shows a significant decrease in max bending moment. This decrease can be attributed to the introduction of a vertical force at the strut location, which provides a bending moment that counteracts the aerodynamic bending moment. The shear force, on the other hand, shows improvements at areas that are further away from the root and trailing edge of the plate. Increases in shear forces at strut locations near the trailing edge are attributed to the wash-in effect that increases the angle of attack of the plate, and thus the lift. The increase near the root of the plate

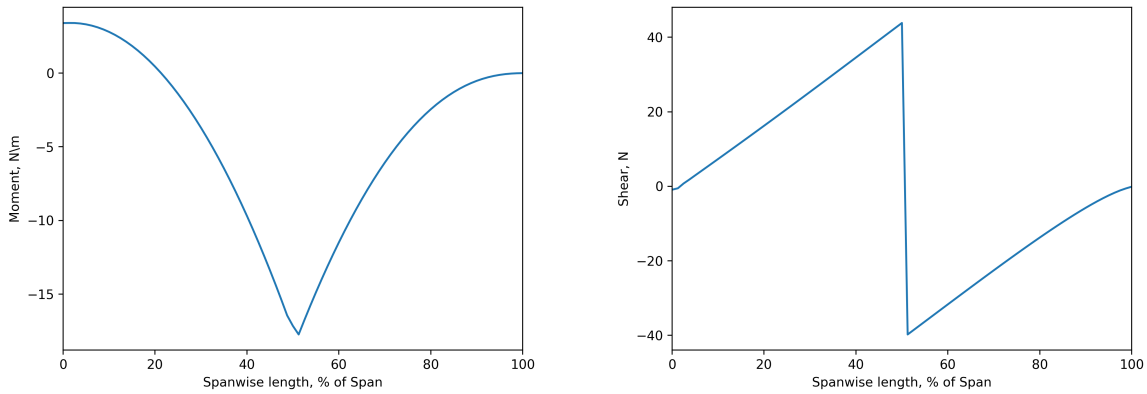

(a) Bending Moment Diagram (b) Shear Force Diagram

Figure 9: Spanwise Moment and Shear Force Diagram for A Strut-Braced Flat Plate

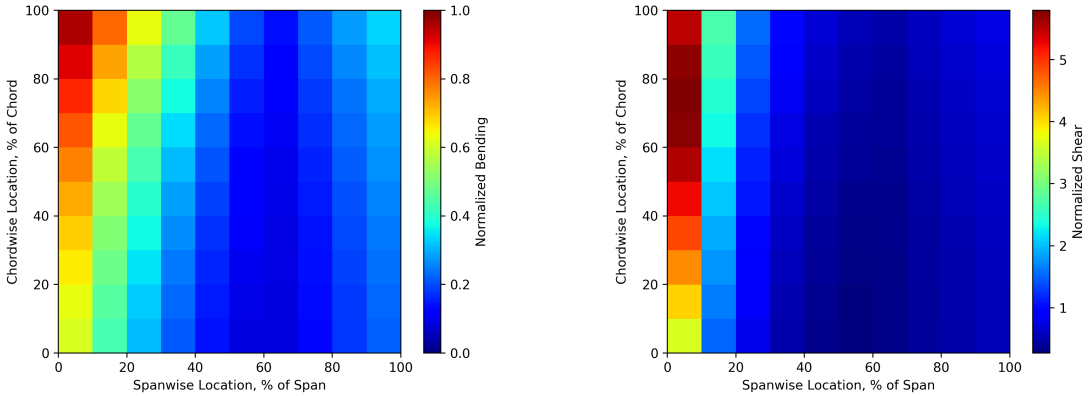

(a) Normalized Max Bending Moment (b) Normalized Max Shear Force

Figure 10: Normalized Structural Performance Parameters By Strut Location

is attributed to an amplification of the forces due to the triangular shape the strut makes with the wing and fuselage and the small angle the strut makes with the fuselage. Strut locations near the mid-span leading edge of the flat plate show improvement in the shear force.

The stability of the strut-braced flat plate is also studied. Areas that show improvement in bending and shear must also satisfy stability at or above the stability of the reference. The critical speed of the strut-braced flat plate is studied and normalized against the reference case. Figure 11 shows the normalized critical speed by strut location on the flat plate.

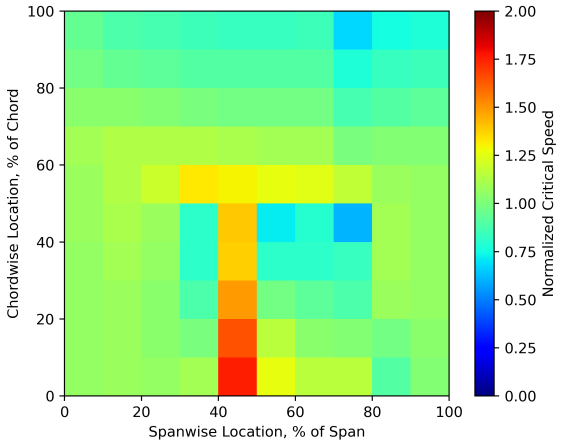

Figure 11: Normalized Critical Speed of the Strut-Braced Flat Plate (A value above 1 shows higher critical speed and is more favorable)

3.1 Geometric Variables Discussion

The optimization of the strut-braced Al-2024 flat plate results in three main conclusions:

- The most favorable boundary condition is the clamped-integral boundary condition, providing optimal structural performance. Other boundary conditions are still viable, with fewer benefits and a narrower range of strut locations on the plate.
- Variation of the strut location on the fuselage with its location on the plate is favorable. Structural and stability benefits are small, and considerations for maintenance, manufacturability, and visual appeal are given priority.
- In terms of strut location, having the strut near the trailing edge significantly reduces aeroelastic critical speed. it is evident that a spanwise location of 40-50%, and 90-100%, with a chordwise location from the leading edge towards 0-50% of the chord, are all viable locations that provide improvement towards structural performance and are stable when compared to the reference case.

These conclusions allow us to minimize the range of variables when designing the strut. In terms of strut location, a strut near the leading edge is not ideal for a few reasons. The strut could interfere with the aerodynamics near the leading edge, causing disturbance to the flow. Moreover, a strut near the leading edge will require special reinforcement of the wing leading to support the load path from the wing to the strut. It will add mechanical and system-level complexities in the event of having a leading-edge device.

A strut further away from the root of the plate is longer and heavier.Therefore, a strut location that minimizes weight, maximizes the flight envelope, and avoids interference with other factors is at 40-50% of the span and at 30-50% of the chord. This results in a 38% improvement in critical speed and a reduction of 81.75% and 56.7% in the max bending moment and shear force, respectively, when compared to the reference cantilever flat plate (no strut).

3.2 D. Ply Orientation of Composite Laminate + Strut Location

Analysis of ply orientation showed that a ply angle of $-22.5°$ and $-45°$ both exhibit significant improvements compared to the reference. It should be noted that the results presented in this section are normalized by the corresponding value of the flat cantilever plate (no strut reference

case), which can be found in table 2. Structural performance was greatly enhanced at all strut locations. Figure 12 illustrates the normalized max bending for both ply orientations, revealing a notable reduction in bending moment at all strut locations. This reduction was attributed to the coupling between bending and torsion of the composite, as indicated by the D_{16} term in the ABD matrix. The coupling introduces a washout effect, leading to reduced bending moments in the plate.

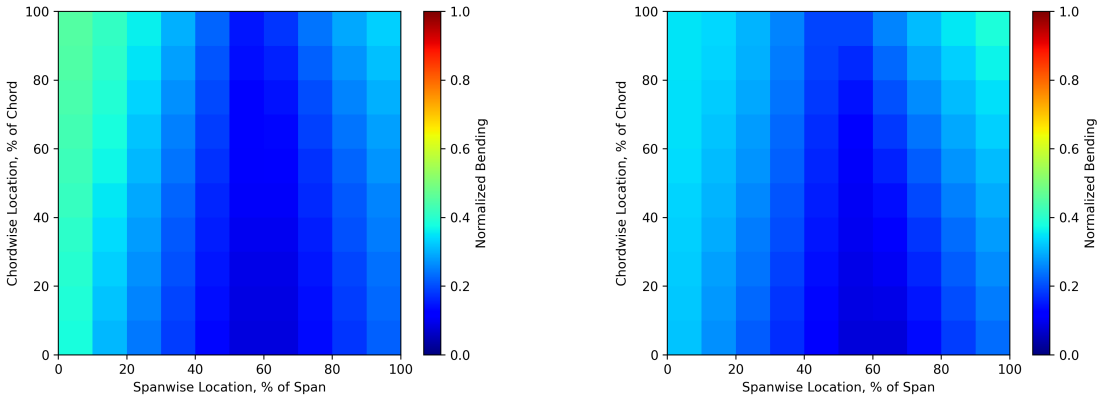

(a) Ply Orientation of $-45°$ (b) Ply Orientation of $-22.5°$

Figure 12: Normalized Max Bending Moment By Strut Location for a Composite Plate

Similarly, the maximum shear force in the flat plate was also affected. Figure 13 illustrates the maximum shear force in the plate by strut location for both optimum ply orientations.

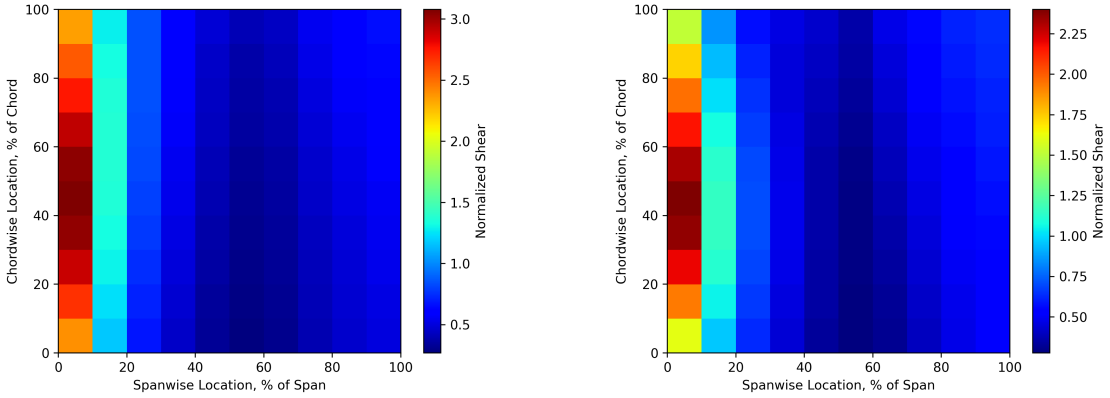

(a) Ply Orientation of $-45°$ (b) Ply Orientation of $-22.5°$

Figure 13: Normalized Max Shear Force By Strut Location for a Composite Plate

The composite plate results in better performance at all strut locations except regions where the strut is close to the root ($0 - 20\%$ of the span). This is attributed to the magnification effect of forces due to the low angle the strut makes with the xz-plane fuselage. Comparison shows that the maximum value of the shear force is lower.

Reductions in max bending moment and max shear force are insufficient without satisfying aeroelastic stability constraints. Viable strut locations and ply angles should reduce max bending moment and max shear force and be at least as aeroelastically stable as the reference case. Figure 14 showcases the critical speed of the composite flat plat with a ply orientation of $-45°$

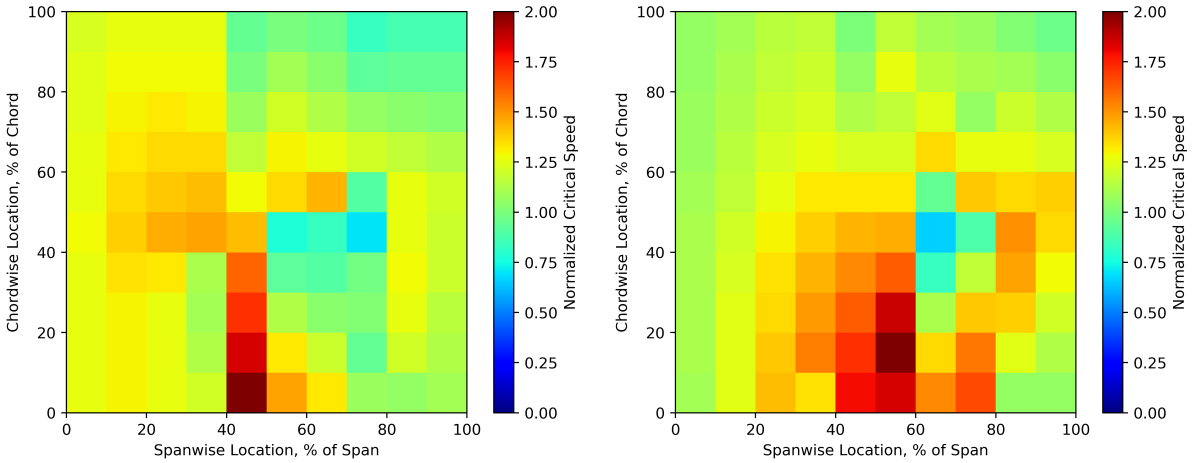

(a) Ply Orientation of $-45°$

(b) Ply Orientation of $-22.5°$

Figure 14: Normalized Critical Speed By Strut Location for a Composite Plate

and $-22.5°$. Stability of the flat plate is improved, and more strut locations are viable. Figure 14 shows the normalized critical speeds of the flat plate for the optimum ply orientations.

Both ply orientations provide a larger range of stable strut locations when compared to the metal flat plate. Ply orientation of $-22.5°$ provides slightly more viable locations than the $-45°$ case. Taking stability and structural performance into account, optimal ranges of strut locations are found. A ply orientation of $-22.5°$ provides structural and stability improvements at spanwise location between $20 - 60\%$ of the span, for all chordwise locations. On the other hand, a ply orientation of $-45°$ is viable at spanwise locations between $20-50\%$ of the span and chordwise locations between $0 - 90\%$ of the chord.

4 CONCLUSIONS AND SUGGESTIONS

Considerations of manufacturability, feasibility, and interference with other systems of an aircraft are important to make a design choice. While the $-22.5°$ composite laminate provides better performance, the $-45°$ is chosen because of the popularity and ease of manufacture of the $-45°$ plies. There is some difference in performance between the two ply orientations, however both provide significant improvements when compared to the reference case. To minimize the weight of the strut, strut locations are narrowed down to $20 - 30\%$ of the span. It should be noted that the chordwise location os narrowed to $30 - 50\%$ of the chord to avoid leading-edge aerodynamics interference, lack of structural support near the leading edge, and possible interference with leading-edge devices. This range of locations provides an improvement of 37% in the critical speed and a reduction of 71.5% and 21.35% in max bending moment and shear force, respectively, when compared to the reference case. For the metal plate the optimum provides a 38% improvement in critical speed, and a reduction of 81.75% and 56.7% in the max bending moment and shear force, respectively.The improvement from the metal optimum is better; however, the metal optimum has a higher weight and a longer strut due to the location of the strut spanwise. This change in spanwise location reduces the weight of the strut from $0.1817, kg$ to $0.0953, kg$, a $47.6\,\%$ reduction. Moreover, a shorter strut is favorable to minimize the aerodynamic effects of the strut on the aircraft. Taking the same location considered for the metal plate ($40 - 50\%$ of the span and between $30 - 50\%$ of the chord) in the composite plate results in an improvement of 51% in the critical speed and a reduction of 84.2% and 61.5% of the max bending moment and shear force, respectively.

Suggestions for expansion on this work include expansion of the design variables (inclusion of novel designs), consideration of manufacturability, higher fidelity studies and rigid body dynamics. Novel designs such as tow-steered composites could show improvements on this design. Higher fidelity study on the wingbox could also be done for higher accuracy and practicality. Considerations of manufacturability for the different strut-boundary conditions will also aid in making a decision as the difference in terms of structural and stability performance is minimal.

5 REFERENCES

[1] Darren Hulst (2022). Boeing Commercial Market Outlook 2022-2041. Available at https://www.boeing.com/resources/boeingdotcom/market/assets/downloads/CMO_2022_Report_FINAL_v02.pdf.

[2] Ran, J. (2017). Aeroelastic tailoring of strut-braced wings. Available at https://repository.tudelft.nl/islandora/object/uuid%3A525970df-c593-40f2-9c59-fb771a774459.

[3] Afonso, F., Vale, J., Oliveira, , et al. (2017). A review on non-linear aeroelasticity of high aspect-ratio wings. *Progress in Aerospace Sciences*, 89, 40–57. ISSN 0376-0421. doi:10.1016/j.paerosci.2016.12.004. Avialable at https://www.sciencedirect.com/science/article/pii/S037604211630077X.

[4] Bras, M., Warwick, S., and Suleman, A. (2022). Aeroelastic evaluation of a flexible high aspect ratio wing UAV: Numerical simulation and experimental flight validation. *Aerospace Science and Technology*, 122, 107400. ISSN 1270-9638. doi:10.1016/j.ast.2022.107400. Available at https://www.sciencedirect.com/science/article/pii/S1270963822000748.

[5] Wright, J. R. and Cooper, J. E. (2014). *Introduction to aircraft aeroelasticity and loads*. Aerospace series. Chichester, West Sussex, England: Wiley, 2nd edition ed. ISBN 978-1-118-70044-0.

[6] P. Chiozzotto, G. (2016). Wing weight estimation in conceptual design: a method for strut-braced wings considering static aeroelastic effects. *CEAS Aeronautical Journal*, 7(3), 499–519. ISSN 1869-5590. doi:10.1007/s13272-016-0204-5.

[7] Ma, Y., Karpuk, S., and Elham, A. (2022). Conceptual design and comparative study of strut-braced wing and twin-fuselage aircraft configurations with ultra-high aspect ratio wings. *Aerospace Science and Technology*, 121, 107395. ISSN 1270-9638. doi:10.1016/j.ast.2022.107395. Available at https://www.sciencedirect.com/science/article/pii/S1270963822000694.

[8] Sohst, M., Lobo do Vale, J., Afonso, F., et al. (2022). Optimization and comparison of strut-braced and high aspect ratio wing aircraft configurations including flutter analysis with geometric non-linearities. *Aerospace Science and Technology*, 124, 107531. ISSN 1270-9638. doi:10.1016/j.ast.2022.107531.

[9] Jason Midkiff (1997). Theory of Finite Element Analysis. Available at https://www.sv.rkriz.net/classes/MSE2094_NoteBook/97ClassProj/num/midkiff/theory.html.

[10] Albano, E. and Rodden, W. P. (1969). A doublet-lattice method for calculating lift distributions on oscillating surfaces in subsonic flows. *AIAA Journal*, 7(2), 279–285. ISSN 0001-1452. doi:10.2514/3.5086. Publisher: American Institute of Aeronautics and Astronautics.

[11] Ab Ghani, A. F., Daud, M., Dhar Malingam, S., et al. (2019). OPTIMISATION OF HYBRID COMPOSITE REINFORCED CARBON AND GLASS USING AHP METHOD. *Defence S and T Technical Bulletin*, 12, 101–112.

COPYRIGHT STATEMENT